Back-analysis of a full-scale dyke stress test with advanced models for soft soils

Muraro, S.; Chao, C.; Su, L.; Jommi, C.

DOI
10.1201/9781003431749-624

Publication date
2024

Document Version
Final published version

Published in
Proceedings of the XVIII ECSMGE 2024

Citation (APA)
Muraro, S., Chao, C., Su, L., & Jommi, C. (2024). Back-analysis of a full-scale dyke stress test with advanced models for soft soils. In N. Guerra, M. Matos Fernandes, C. Ferreira, A. Gomes Correia, A. Pinto, & P. Sêco e Pinto (Eds.), *Proceedings of the XVIII ECSMGE 2024: Geotechnical Engineering Challenges To Meet Current And Emerging Needs Of Society* (pp. 3176-3181). Article 624 CRC Press / Balkema - Taylor & Francis Group. https://doi.org/10.1201/9781003431749-624

Proceedings of the XVIII ECSMGE 2024
GEOTECHNICAL ENGINEERING CHALLENGES
TO MEET CURRENT AND EMERGING NEEDS OF SOCIETY

ISBN 978-1-032-54816-6
DOI 10.1201/9781003431749-624

ECSMGE 24
XVIII EUROPEAN CONFERENCE ON SOIL MECHANICS AND GEOTECHNICAL ENGINEERING

Back-analysis of a full-scale dyke stress test with advanced models for soft soils

Rétro-analyse d'un essai de contrainte sur digue en grandeur réelle à l'aide de modèles avancés pour les sols mous

S. Muraro*, C. Chao
Delft University of Technology, Delft, The Netherlands

L. Su, C. Jommi
Delft University of Technology, Delft, The Netherlands
Politecnico di Milano, Milano, Italy

**s.muraro@tudelft.nl*

ABSTRACT: Advanced models for soft organic layers encountered in the shallow subsoils in the Netherlands have been developed recently at TU Delft. The models are based on high-quality laboratory data on peats and soft organic clays. The constitutive effort mostly focussed on some partially unexplored features, such as the role of fibres, extension stress conditions, and the dependence of hardening on deviatoric plastic strains, besides anisotropy. Although the models have proven to be able to reproduce and predict the behaviour over a variety of triaxial probe tests, validation at the field scale is lagging behind. On the one hand, field soil response encompasses diverse stress paths and histories not replicable in the laboratory. On the other hand, the role of the advanced features introduced in the models on the engineering structure response needs to be quantified. We back-analyse a well-documented full-scale test performed in the Netherlands, the Leendert de Boerspolder stress test, where the role of different soft soil layers both on the pre-failure and failure response has been investigated. Comparison between numerical simulations and available monitoring data is used to demonstrate the contribution of advanced models to the understanding of the engineering response of soft soils.

RÉSUMÉ: Des modèles avancés pour les couches organiques molles trouvées dans les sous-sols superficiels aux Pays-Bas ont été développés récemment à TU Delft. Les modèles sont basés sur des données de laboratoire de haute qualité sur les tourbes et les argiles organiques molles. L'effort constitutif s'est principalement concentré sur certaines caractéristiques partiellement inexplorées, telles que le rôle des fibres, les conditions de contrainte d'extension et la dépendance de l'écrouissage aux déformations plastiques déviatoriques, en plus de l'anisotropie. Bien que les modèles se soient avérés capables de reproduire et de prédire le comportement lors d'une variété d'essais à la sonde triaxiale, la validation à l'échelle du terrain est à la traîne. D'une part, la réponse du sol sur le terrain englobe diverses chemins de contraintes et histoires qui ne peuvent être reproduites en laboratoire. D'autre part, le rôle des caractéristiques avancées introduites dans les modèles sur la réponse de la structure d'ingénierie doit être quantifié. Nous rétro-analysons un essai en échelle réelle bien documenté réalisé aux Pays-Bas, l'essai de contrainte de Leendert de Boerspolder, où le rôle de différentes couches de sol mou a été étudié à la fois sur la réponse avant rupture et sur la réponse à la rupture. La comparaison entre les simulations numériques et les données de surveillance disponibles est utilisée pour démontrer la contribution des modèles avancés à la compréhension de la réponse d'ingénierie des sols mous.

Keywords: Soft soils; advanced constitutive modelling; numerical simulation; case-history.

1 INTRODUCTION

The Netherlands relies on an extensive network of primary and secondary flood defence embankments. Many dykes, especially in the western part of the country, lie on thick deposits of peat and organic clay, prone to settlement and shear deformation. Assessing the serviceability and safety of these dykes is challenging due to the complex behaviour of soft soils under general stress paths.

To better understand the engineering response of these soils, advanced models for the soft organic layers encountered in the shallow subsoils in the Netherlands have been recently developed at TU Delft. These models include non-associated plastic flow rule, anisotropy described by a rotational hardening law, and a generalised hardening rule, which depends on both deviatoric and volumetric plastic strains. While the models have proven to be able to replicate the

response of the soils in a variety of triaxial stress paths, validation at the field scale is lagging behind.

In this study, we back-analyse a well-documented full-scale stress test performed in the Netherlands, the Leendert de Boerspolder stress test (De Gast, 2020; Jommi et al., 2021). Finite element simulations incorporating standard and new advanced models for soft soils are carried out, and the results of the numerical simulations are compared with in-situ monitoring data.

2 OVERVIEW OF THE FIELD TEST

The Leendert de Boerspolder dyke was a regional dyke located north of Leiden (Figure 1). Under service conditions, the water levels in the canal and polder were regulated with little variations: the canal regulating system kept the water level on the canal side at constant h = - 0.6 m NAP, in which the NAP (Normaal Amsterdams Peil) is used as the reference for the vertical coordinate. On the polder side, it was managed by pumping stations at h = - 2.3 m NAP.

Figure 1. Plane view of the test area at the Leendert de Boerspolder before the start of the failure test (https://www.stabialert.nl/nl/projecten/ldeb-polder/).

The stress test consisted of a series of excavation and dewatering stages operated at the toe of the dyke to induce the failure. The schematisation of the cross-sectional view of the dyke, along with the geometry of the excavations and the position of monitoring instrumentation, are presented in Figure 2.

In the first stage, a trench was excavated at the toe of the dyke while maintaining the water level in the trench unchanged. Subsequently, the water level was lowered by one meter in two steps. At the end of the first stage, the water was refilled back to the same water level as at the start. Similar operations were performed in the following second and third excavation stages, with a more extensive portion of soil being removed. The dyke failed during the last dewatering step between Section Centre and Section South (Figure 1).

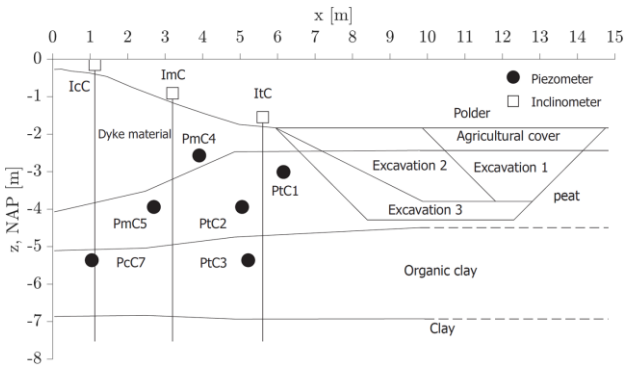

Figure 2. Schematisation of the central cross-sectional profile of the dyke and monitoring instrumentation.

2.1 Subsoil properties

To characterise the soil layers at the test site, an extensive site and laboratory investigation program was carried out including CPTu, triaxial, simple shear and oedometer tests on undisturbed soil samples (Ponzoni, 2017). The reconstructed soil profile consists of: (i) highly heterogeneous dyke material; (ii) peat layer with a varying thickness between 1.5 – 2.5 m; (iii) organic clay deposit with a thickness of about 2.0 m; (iv) deep clay layer above the Pleistocene sand. The dry density, void ratio, hydraulic conductivity, and over-consolidation ratio estimated from oedometer and triaxial tests on undisturbed samples, are summarised in Table 1. For the peat layer, the dependence of the hydraulic conductivity on the void ratio is reported by Zhao and Jommi (2023). For the in-situ void ratio, the hydraulic conductivity is in the range between 10^{-6} m/s to 10^{-7} m/s.

Table 1. Material properties for each layer.

Layer	ρ_d [kg/m^3]	e [-]	k [m/s]	OCR [-]
Dyke	1290	1.3	5×10^{-8}	1.0-1.6
Peat	150	9.0-13.0	$k\,(e)$	1.0-3.0
Organic clay	610	2.8	5×10^{-9}	1.0-3.0
Clay	900	1.0	5×10^{-9}	1.0

2.2 Monitoring instrumentation

The in-situ instrumentation was designed with the two primary purposes of providing sufficient data on the pre-failure response of the system, during excavation, dewatering, refilling, and collecting as much information as possible during the failure. It included: (i) 25 piezometers; (ii) 5 automatic two-axis inclinometers; and (iii) 9 vertical rod-type extensometers allowing to automatically record settlement and heave of the different soil layers. The sensors were installed at three cross-sections along the longitudinal direction, namely Section North, Centre, and South. Figure 2 reports the

position of the instrumentation in the Section Centre which was the most instrumented one.

3 CONSTITUTIVE MODELS

Different constitutive models are chosen for the different soil layers. In all the numerical simulations, the dyke material and the deep clay layer are modelled as linear-elastic perfect plastic material with the Mohr-Coulomb failure criterion. For the peat layer and the organic clay layer, the results of the two analyses are compared. In the first one, the Modified Cam Clay (MCC, Roscoe and Burland, 1968) was used. The second one was run adopting the advanced models developed at TU Delft.

For the peat layer, the model proposed by Muraro and Jommi (2021) is adopted. It includes a non-associated isotropic yield surface and plastic potential and a mixed volumetric and distortional hardening law derived from triaxial probe tests. For the organic clay layer, the recently proposed model by Chao (2024) is adopted. The model extends the generalised expression of yield locus proposed by McDowell and Hau (2003) to account for anisotropy. The evolution of anisotropy in the model is described by an amended version of the rotational hardening rule proposed by Dafalias and Taiebat (2013) to better capture the stress-strain response observed in the extension domain. The proposed expression for the rate of evolution of the rotation hardening variable, α, and the corresponding asymptotic values, α_b, are defined as

$$\delta\alpha = \langle L \rangle c p_{atm} \frac{p'}{p'_c} (\alpha_b - \alpha) \tag{1}$$

$$\alpha_b = \begin{cases} \frac{M_{g,c}}{z_c}\left[1 - \exp\left(-s\frac{|\eta|}{M_{g,c}}\right)\right]^y, \eta \geq 0 \\ -\frac{M_{g,e}}{z_e}\left[1 - \exp\left(-s\frac{|\eta|}{M_{g,e}}\right)\right]^y, \eta < 0 \end{cases} \tag{2}$$

with $M_{g,c}$, $M_{g,e}$ critical stress ratio in compression and extension, η stress ratio, p_{atm} atmospheric pressure, p' mean effective stress, p'_c preconsolidation stress, L plastic multiplier, and z_e, z_c, c, s, y model constants. Both constitutive models are implemented in ABAQUS in UMAT subroutines.

The model parameters adopted in the numerical simulations for each soil layer and summarised in Table 2, Table 3, and Table 4 were calibrated on triaxial stress probe tests (Ponzoni, 2017; Muraro and Jommi, 2021; Chao 2024). The compression parameters for the peat and organic clay in the new models remain as in the MCC.

For the organic clay, the constants of the rotational hardening rule (Equations (1) and (2)) are z_c = 1.6, z_e = 1.2, c = 50, s = 2.2, y = 2. The initial inclination of the yield locus and plastic potential was determined following the procedure described by Dafalias et al. (2006), assuming K_0 conditions for the stress state of the sample in the field. The calculated initial inclination is α_i = 0.50.

Table 2. Input parameters for dyke and deep clay.

Layer	E [kPa]	ν [-]	φ [°]	ψ [°]	c [kPa]
Dyke	5600	0.3	30.0	3.0	5.0
Clay	5200	0.3	31.0	6.0	5.0

Table 3. Input parameters for peat and organic clay modelled with the MCC.

Layer	κ^* [-]	ν [-]	λ^* [-]	M [-]	K [-]
Peat	0.08	0.3	0.36	1.75	0.8
Organic clay	0.009	0.2	0.09	1.42	0.8

Table 4. Input parameters for peat and organic clay modelled with the new advanced models.

Layer	$M_{g,c}$ [-]	$M_{g,e}/M_{g,c}$ [-]	$M_{f,c}$ [-]	χ_f [-]	χ_g [-]
Peat	1.75	0.80	1.5	2.0	0.98
Organic clay	1.42	0.80	1.0	1.25	2.0

4 NUMERICAL MODEL

The field stress test is modelled as a 2D plane-strain, hydro-mechanical coupled problem in the finite element software ABAQUS, and its geometry is presented in Figure 3. The model consists of 10128 type "CPE8RP" elements.

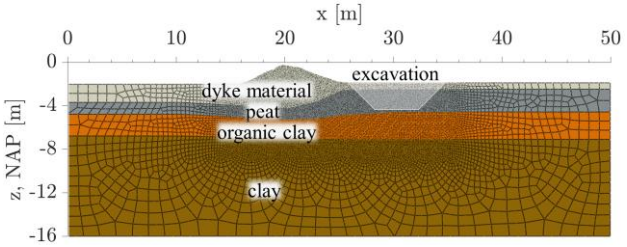

Figure 3. Geometry and mesh of the FE model.

4.1 Boundary and initial conditions

The following boundary constraints are imposed: (i) the two lateral vertical boundaries are fixed in the horizontal direction; (ii) the lower boundary is fixed in the horizontal and vertical directions; (iii) hydrostatic

pore pressure profile is applied to the lateral boundaries corresponding to the water level in the canal and the water table at the polder; (iv) drainage-only flow condition is imposed on the outer slope of the dyke.

To simulate the excavation process underwater the module "Model Change" is used which reduces gradually the forces/fluxes exerted by the region to be removed. In the dewatering step, a drainage-only flow condition is applied to the lateral boundaries of the excavation trench, which enables the reduction of pore pressure to the desired value. The boundary conditions applied during the excavation and dewatering steps are displayed in Figure 4.

To reflect the different stress history and stress levels in the foundation layers, an initial profile of OCR changing in the x-direction is assigned to the peat and the organic clay layer as shown in Figure 5. The chosen OCR profile simplifies the interpolation of oedometer data from undisturbed samples.

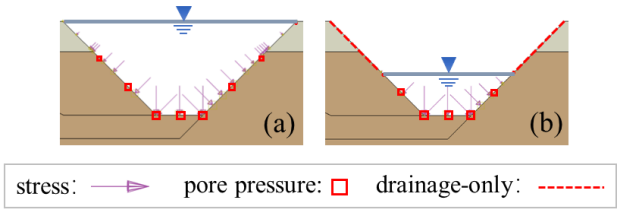

Figure 4. Schematization of the boundary conditions: (a) at the end of excavation; (b) at the end of the dewatering.

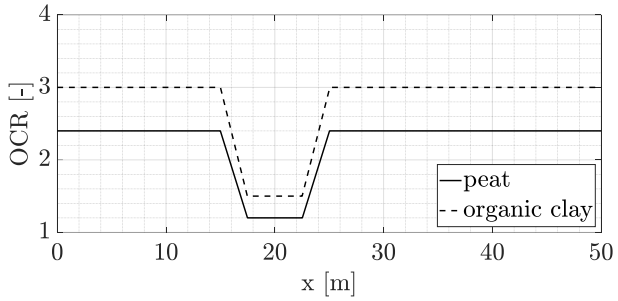

Figure 5. OCR profile in peat and organic clay layer.

4.2 Analysis phases

The analysis steps defined in the numerical simulations are presented in Table 5. The so-called "geostatic step" at the beginning of the analysis is used to establish equilibrium before the loading stage with the applied loads, boundary conditions and initial conditions. Each other step replicates one operation of the stress test. It should be noted that the third dewatering step (on 10-14, Table 5) involved three sub-steps, each pumping 0.5 meters of water with a 30-minutes consolidation period in between.

Table 5. Analysis steps in the simulations.

Operation	Label	Start (mm-dd)	Duration (h)
Initial State	-	-	-
Excavation 1	E1	09-28 09:20	6.9
Dewatering 1	D1	09-30 09:20	2.7
Filling 1	F1	10-01 12:45	1.3
Excavation 2	E2	10-05 08:00	9.5
Dewatering 2	D2	10-07 09:05	4.3
Filling 2	F2	10-08 08:00	2.1
Excavation 3	E3	10-12 07:20	9.4
Dewatering 3	D3	10-14 00:30	5.6

5 NUMERICAL RESULTS

In this section, the numerical results in terms of horizontal displacements and pore pressure response are presented and compared with in-situ measurements. The attention is given to the prediction of different constitutive models, MCC and the new advanced models for peat and organic clay layers.

5.1 Horizontal displacements

Figure 6 shows the resultant displacement predicted at the end of the final dewatering step from both the MCC and the advanced models. Both simulations predict a failure mechanism characterized by the outward bulging of the peat layer at the toe. This pattern, typical for peat (Landva and La Rochelle, 1983) is consistent with the field monitoring data.

Figure 7 presents the numerical predictions and the inclinometer measurements installed at the crest (IcC), mid-slope (ImC) and toe (ItC). The layering is indicated with the letters D, P, and OC which stand for dyke material, peat and organic clay. The data for the first, second, and third dewatering steps are plotted in black, red, and blue, respectively. The comparison in Figure 7 shows better qualitative and quantitative prediction of the horizontal displacement profile by the new advanced models compared to the MCC. Very good agreement is observed for the organic clay layer at the toe and mid-slope of the dyke where the MCC underestimates the magnitude of the displacement. Reconstruction of the failure mechanics from in-situ measurements revealed that the failure originated initially in the organic clay layer at the toe (Jommi et al., 2021). It is worth remarking that the inclinometer ImC was working down to – 5.5 m (NAP) only.

The benefit of the new models is also evident for the peat layer with a bulging profile predicted at the toe very close to the observed one. The simulation with the advanced models yields a maximum displacement of 0.086 m, compared to 0.065 m predicted by the

MCC, thus very close to the observed one, 0.1 m. The difference in predicted and observed displacements increases towards the upper peat layer, likely due to different mechanical properties of the surficial and deep peat layer as indicated by laboratory tests. Good agreement is also observed in the peat layer at the mid-slope of the dyke (ImC). For the inclinometer IcC, the final horizontal displacement is slightly overestimated. Laboratory tests indicated slightly stiffer peat and organic clay samples below the crest of the dyke compared to the polder side.

It is worth noticing that the difference between the MCC and the new models predictions is not evident in the first two dewatering stages but becomes clear in the last dewatering stage (blue lines in Figure 7). In the early dewatering stage, the soil stress state remains mostly inside the elastic domain, given the initial OCR profile. The difference becomes dominant as the stress state enters the plastic domain. The initial yield locus rotation and progressive reorientation during the last stages of dewatering improved the predictions for the organic clay layer, particularly at the toe of the dyke. Additionally, adopting a non-associated flow rule calibrated on experimental data helped to better replicate the plastic deformation mode in the peat layer.

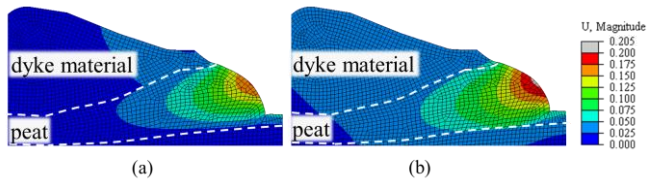

Figure 6. Displacement contour at the end of the third dewatering step: (a) MCC; (b) new models (units in m).

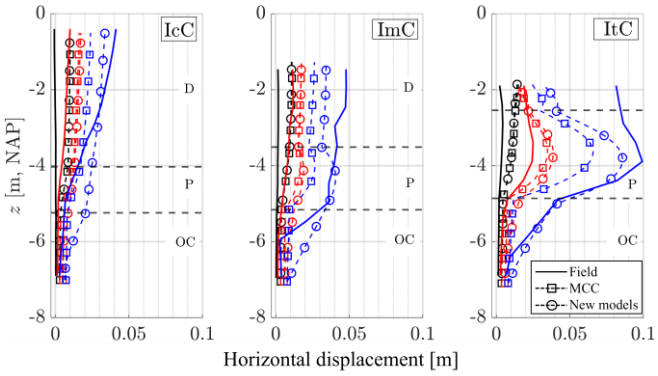

Figure 7. Measured and simulated horizontal displacement along inclinometer IcC, ImC, and ItC at the end of three dewatering stages.

5.2 Hydraulic response

The hydraulic response predicted by the numerical simulations and the comparison with field measurements is presented in Figure 8 in terms of variation of the excess pore pressure at piezometers PtC1, PtC2, PtC3, and PmC4 located at the toe of the dyke and in the dyke material (Figure 1) throughout the different steps. The timing of each operation is indicated by the labels E, D, and F as indicated in Table 5. The excess pore pressure is calculated based on the pore pressure before the first excavation stage.

The changes in pore water pressure during the initial excavation and dewatering step (E1, D1) are minimal due to the limited extent of excavation and the relatively small drawdown during the first operation stage. Small differences are observed in the numerical prediction for PmC4 during refilling after the first excavation and dewatering, with the new models better replicating the measurements.

The reduction in pore water pressure observed during the second and third excavation and dewatering phases (E2, D2, E3, and D3) is well captured.

Despite the difference in the displacement profile previously outlined, the variation of pore water pressure between the simulations, using the MCC and advanced models, is nearly identical. This suggests that the compressibility coefficient dominates the pore pressure response. In addition, it is relevant to mention that the dyke failure took place between Section Centre, here considered as representative cross-section, and Section South. Additional examination of the piezometer measurements at both Section South and Section North will be necessary to fully assess the model predictions in terms of hydraulic response.

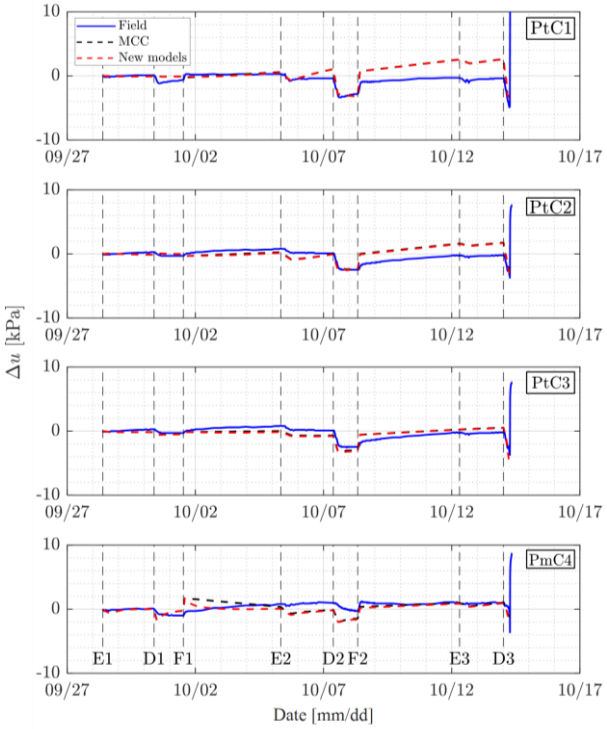

Figure 8. Measured and simulated time history of excess pore pressure at piezometer PtC1, PtC2, PtC3, and PmC4.

6 DISCUSSION AND CONCLUSIONS

This study presents a comparison between finite element simulations and in-situ measurements of a well-documented case study of a full-scale dyke stress test conducted on a regional dyke in the Netherlands. Particular attention is given to analysing the behaviour of the foundation layers consisting of peat and organic clays. Hydro-mechanical coupled finite element simulations are conducted with both traditional and new advanced constitutive models developed at TU Delft to better capture the complex behaviour of organic soft soils.

The numerical simulations show the benefits of the advanced models in better replicating both qualitatively and quantitatively the observed displacement field. In particular, the new models show a more diffusive displacement profile in the organic clay layer, where failure originated and a more pronounced lateral bulging profile very characteristic of peat.

The evolution of pore water pressure at different positions is well captured, with variations nearly identical in simulations using both MCC and advanced models possibly due to the dominant role of the compressibility coefficient in the overall volumetric response.

The comparison between the predicted displacement field along the entire cross-section profile with the in-situ data and laboratory data suggests possible variations of the compression coefficients within the foundation layers along the horizontal direction which should be accounted for a further refinement of the geotechnical model used in the numerical simulations. In addition, given the very small effective stress level which characterises regional dykes on soft soils, a proper initialisation of the in-situ stress state and OCR profile is of paramount importance to assess the engineering response of geo-infrastructure on soft soils.

ACKNOWLEDGEMENTS

The financial support of STOWA and the Dutch organisation for scientific research NWO, under the project “Reliable Dykes 13864“ is acknowledged. Thanks are due to Tom de Gast, who managed the design of the stress test in the field as part of his PhD research.

REFERENCES

Chao, C.Y. (2024). A comprehensive journey on Dutch organic clays. From element testing through constitutive modeling towards a novel cyclic multidirectional shear device. PhD Thesis, Delft University of Technology.

Dafalias, Y. F. and Taiebat, M. (2013). Anatomy of rotational hardening in clay plasticity. Geotechnique, 63(16), pp. 1406-1418. https://doi.org/10.1680/geot.12.P.197.

De Gast, T. (2020). Dykes and Embankments: a Geostatistical Analysis of Soft Terrain. PhD Thesis, Delft University of Technology, Delft. https://doi.org/10.4233/uuid:4ce3b4ec-0a6a-4886-9a82-5945a1f9ea50.

Jommi, C., Chao, C.Y., Muraro, S., and Zhao, H.F. (2021). Developing a constitutive approach for peats from laboratory data. Geomechanics for Energy and the Environment, 27, pp. 100-220. https://doi.org/10.1016/j.gete.2020.100220.

Landva, A.O., and La Rochelle, P. (1983). Compressibility and Shear Characteristics of Radforth Peats. ASTM International. pp. 157-191. https://doi.org/10.1520/STP37341S.

McDowell, G.R., and Hau, K.W. (2003). A simple non-associated three surface kinematic hardening model. Geotechnique, 53(4), pp. 433-437. https://doi.org/10.1680/GEOT.2003.53.4.433.

Muraro, S., and Jommi, C. (2021). Pre-failure behaviour of reconstituted peats in triaxial compression. Acta Geotechnica, 16(3), pp. 789-805. https://doi.org/10.1007/S11440-020-01019-2.

Ponzoni, E. (2017). Historical constructions on natural silty soils accounting for the interaction with the atmosphere. PhD thesis, Università degli Studi di Brescia.

Roscoe, K.H., and Burland, J.B. (1968). On the generalized stress-strain behaviour of wet clay. In Engineering plasticity, pp. 535-609. Cambridge University Press.

Zhao, H., and Jommi, C. (2023). Consequences of drying on the engineering properties of fibrous peats: compression behaviour. Canadian Geotechnical Journal, 60(4), pp. 438–452. https://doi.org/10.1139/cgj-2020-0086.